

GPS Dropwindsonde Wind Profiles in Hurricanes and Their Operational Implications

JAMES L. FRANKLIN

Tropical Prediction Center, National Hurricane Center, NOAA/National Weather Service, Miami, Florida

MICHAEL L. BLACK

Hurricane Research Division, NOAA/Atlantic Oceanographic and Meteorological Laboratory, Miami, Florida

KRYSTAL VALDE

Tropical Prediction Center, National Hurricane Center, NOAA/National Weather Service, Miami, Florida

(Manuscript received 9 June 2002, in final form 2 October 2002)

ABSTRACT

The recent development of the global positioning system (GPS) dropwindsonde has allowed the wind and thermodynamic structure of the hurricane eyewall to be documented with unprecedented accuracy and resolution. In an attempt to assist operational hurricane forecasters in their duties, dropwindsonde data have been used in this study to document, for the first time, the mean vertical profile of wind speed in the hurricane inner core from the surface to the 700-hPa level, the level typically flown by reconnaissance aircraft. The dropwindsonde-derived mean eyewall wind profile is characterized by a broad maximum centered 500 m above the surface. In the frictional boundary layer below this broad maximum, the wind decreases nearly linearly with the logarithm of the altitude. Above the maximum, the winds decrease because of the hurricane's warm core. These two effects combine to give a surface wind that is, on average, about 90% of the 700-hPa value. The dropwindsonde observations largely confirm recent operational practices at the National Hurricane Center for the interpretation of flight-level data. Hurricane wind profiles outside of the eyewall region are characterized by a higher level of maximum wind, near 1 km, and a more constant wind speed between 700 hPa and the top of the boundary layer. Two factors that likely affect the eyewall profile structure are wind speed and vertical motion. A minimum in surface wind adjustment factor (i.e., relatively low surface wind speeds) was found when the wind near the top of the boundary layer was between 40 and 60 m s⁻¹. At higher wind speeds, the fraction of the boundary layer wind speed found at the surface increased, contrary to expectation. Low-level downdrafts, and enhanced vertical motion generally, were also associated with higher relative surface winds. These results may be of interest to engineers concerned with building codes, to emergency managers who may be tempted to use high-rise buildings as a "refuge of last resort" in coastal areas, and to those people on locally elevated terrain. The top of a 25-story coastal high-rise in the hurricane eyewall will experience a mean wind that is about 17% higher (or one Saffir-Simpson hurricane-scale category) than the surface or advisory value. For this reason, residents who must take refuge in coastal high-rises should generally do so at the lowest levels necessary to avoid storm surge.

1. Introduction

Obtaining observations that describe the detailed inner-core kinematic structure of a tropical cyclone has, understandably, proven to be a challenging exercise. Research and reconnaissance aircraft in situ measurements have been the primary tools for such studies over much of the past 50 years. This instrumentation has provided a wealth of information over the years, with a large body of literature, including Hawkins and Rubsam's (1968) analysis of multilevel aircraft data, Wil-

loughby et al.'s (1982) description of concentric eyewalls, and Jorgensen's (1984) schematic of the core of Hurricane Allen, forming the basis for much of our current understanding of the inner structure and workings of tropical cyclones. In more recent studies, airborne Doppler radars have helped to provide more comprehensive descriptions of tropical cyclone structure (e.g., Marks and Houze 1987; Marks et al. 1992). Despite all the progress, comprehensive observations of the hurricane boundary layer have been especially hard to come by, because of both safety considerations and instrumentation limitations. In particular, reliable estimation of a parameter of special interest to the tropical cyclone forecaster and the public has remained elusive—namely, the cyclone's maximum sustained surface (10 m) wind.

Corresponding author address: James L. Franklin, Tropical Prediction Center, National Hurricane Center, NOAA/NWS, 11691 SW 17th St., Miami, FL 33165-2149.
E-mail: james.franklin@noaa.gov

Aircraft reconnaissance observations in hurricanes are typically obtained from the relative safety found at the 700-hPa flight level, with lower flight altitudes, ranging from 305 m (1000 ft) to 850 hPa, employed in weaker systems. From these observations aloft, the forecaster must estimate the surface winds. It is clear that to estimate the surface wind confidently from the flight-level data, one must have knowledge of the vertical profile of wind in the hurricane core.

The general wind structure, in which a maximum in wind speed is found near the top of a frictional boundary layer, with decreasing winds aloft because of the thermal wind associated with the hurricane's warm core, has been long understood. In the past, however, measurements have been inadequate to address directly the problem of "adjusting" flight-level reconnaissance wind measurements in the hurricane eyewall to the surface. Numerous rawinsonde studies of tropical cyclones exist (e.g., Frank 1977), but with little data from the eyewall region. Airborne Doppler radars measure winds in the eyewall well, albeit with inherent smoothing and not below an altitude of about 300–500 m (e.g., Marks et al. 1992). Research aircraft have occasionally made "spiral ascent" soundings in hurricanes, but not in the eyewall because of flight-safety considerations. Dropwindsondes based on Omega navigation (Franklin and Julian 1985) rarely worked in heavy precipitation and in any event did not measure winds below about 500 m.

In a study that specifically addressed the issue of reconnaissance wind adjustments, Powell and Black (1990) recommended that an adjustment factor of 63%–73% be used to reduce 700-hPa wind speeds to the surface, based on comparisons of flight-level and buoy data (again, mostly outside of the eyewall). Operational practices at the National Hurricane Center (NHC) have varied over time; in recent years surface winds have typically been taken to be 80%–90% of the flight-level wind. This practice was motivated largely by the assumption that strong convective motions in the hurricane eyewall would be particularly effective at transporting high-momentum air to the surface layer. Use of these relatively high ratios has periodically resulted in criticism of NHC intensity estimates.

The development of the global positioning system (GPS)-based dropwindsonde (Hock and Franklin 1999) has made it possible to obtain vertical profiles of wind and thermodynamic parameters within nearly all portions of the hurricane with unprecedented accuracy and resolution. In 1997, National Oceanic and Atmospheric Administration (NOAA) hurricane research aircraft began deploying these sondes¹ in the hurricane eyewall and surrounding regions. The Air Force Reserve Command (AFRC) followed suit in 1998, heralding a new era in aerial hurricane reconnaissance.

In this study, we present an analysis of three years

(1997–99) of dropsonde data that document the lower-tropospheric vertical variation of winds in the hurricane core region, extending the preliminary findings of Franklin et al. (2000), and Black and Franklin (2000). Individual dropsonde profiles from the eyewalls of several hurricanes are shown to illustrate the variety of structures observed. Mean profiles are constructed for the eyewall and surrounding outer-core regions, and empirical relationships (adjustment factors) to convert winds from one level to another are determined. Several stratifications of the data are performed to help to identify those factors that control the variation in the adjustment factors.

2. Data

Hock and Franklin (1999) provide a complete description of the GPS dropwindsonde. Developed by the National Center for Atmospheric Research in the mid-1990s in a joint effort with NOAA and the German Aerospace Research Establishment, the new sonde represents a radical departure in design and performance from previous generations. The sonde is smaller (diameter and length of 7 and 41 cm, respectively) and lighter (~400 g) than its predecessors. Narrow bandwidth data transmission and an antenna redesign permit the sonde's signals to be received in environments of enhanced electrical activity, where previous sondes performed poorly. The thermodynamic sensors are modern, capacitive sensors manufactured by Vaisala Oy of Helsinki, Finland. Omega-based wind-finding has been replaced by GPS satellite navigation. With a sampling rate of 2 Hz and a near-surface fall rate of 11–12 m s⁻¹, the vertical resolution of both the wind and thermodynamic observations from the sonde in the lower troposphere is approximately 5 m. An error analysis of the wind data by Hock and Franklin indicates that the precision (repeatability) of the wind observations is ~0.2 m s⁻¹, with an absolute accuracy of 0.5–2.0 m s⁻¹.

The dataset for this study consists of 630 hurricane dropsonde profiles obtained during the 1997–99 seasons by NOAA and AFRC hurricane-hunter aircraft. The vast majority of these profiles were obtained in the Atlantic tropical cyclone basin, with a small number coming from reconnaissance or research flights in the eastern and central North Pacific basins. The hurricanes composing this sample are Guillermo and Erika in 1997; Bonnie, Danielle, Georges, Mitch, Lester, and Madeline in 1998; and Bret, Dennis, Floyd, Gert, Irene, Jose, Lenny, Dora and Eugene in 1999 (Table 1). A wide range of hurricane intensities, from 65 to 155 kt (33–80 m s⁻¹), is covered by this sample. Of the 630 profiles, 429 were from the hurricane eyewall, and the remaining 201 were outside the eyewall but within about 300 km of the center. Assignment of particular soundings to the "eyewall" or "outer vortex" categories was to some extent subjective but was based on examination of individual concurrent flight-level radial wind profiles and,

¹ In this paper, the terms dropwindsonde, dropsonde, and sonde will be used interchangeably.

TABLE 1. Sample of GPS dropwindsondes used in this study. Eastern and central North Pacific hurricanes are indicated by EP and CP, respectively.

Hurricane	No. of eyewall soundings	No. of outer-vortex soundings	Obs period (eyewall soundings)
Guillermo (EP)	9	69	1948–2354 UTC 3 Aug 1997
Erika	26	11	1725 UTC 7 Aug–2240 UTC 8 Aug 1997
Bonnie	56	83	1959 UTC 23 Aug–0337 UTC 28 Aug 1998
Danielle	26		1140 UTC 27 Aug–0250 UTC 1 Sep 1998
Georges	59	38	1718 UTC 19 Sep–1309 UTC 28 Sep 1998
Mitch	50	1	0744 UTC 24 Oct–2302 UTC 28 Oct 1998
Lester (EP)	6		1824 UTC 16 Oct–1419 UTC 17 Oct 1998
Madeline (EP)	2		2025–2033 UTC 18 Oct 1998
Bret	22		1709 UTC 21 Aug–2338 UTC 22 Aug 1999
Dennis	53		0513 UTC 26 Aug–1825 UTC 4 Sep 1999
Floyd	81		2129 UTC 9 Sep–0723 UTC 16 Sep 1999
Gert	7		0830 UTC 16 Sep–0548 UTC 21 Sep 1999
Irene	2		0543–0758 UTC 18 Oct 1999
Jose	1		1328 UTC 20 Oct 1999
Lenny	23		0747 UTC 15 Nov–0728 UTC 19 Nov 1999
Dora (CP)	5		1740 UTC 15 Aug–1328 UTC 17 Aug 1999
Eugene (CP)	2		1733–1933 UTC 12 Aug 1999

where available, airborne radar reflectivity imagery. Considerable weight was given to the comments of the flight meteorologist, who had access to real-time aircraft radar imagery. Sondes were classified as eyewall if they were identified as such by the flight meteorologist or if they were clearly released within the hurricane's main band of strongest winds or highest reflectivities. The sample does not include sondes released in the eye, even if they later intersected the eyewall at low levels as they descended.

Figure 1 shows the locations of the Atlantic-basin eyewall soundings. The sample is seen to include hurricanes in the Caribbean Sea and Gulf of Mexico, although the preponderance of the data are from the western Atlantic. There are very little data north of 35°N, so the results presented here will likely not be appropriate for storms over cooler waters affecting the northeastern United States. Figure 2 shows the eyewall

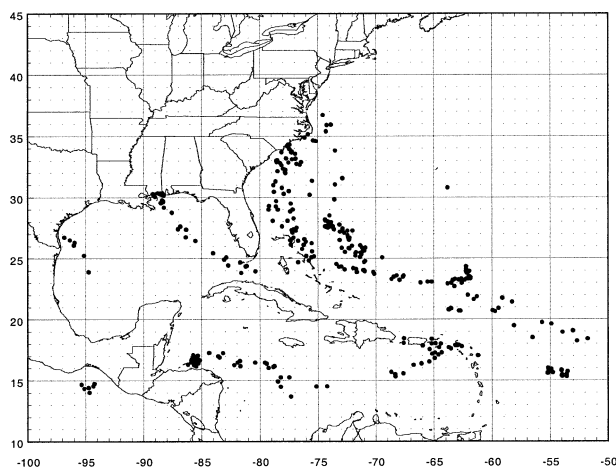


FIG. 1. Locations of Atlantic-basin eyewall dropsondes (filled circles) during the 1997–99 hurricane seasons used in this study.

sounding locations relative to the position of the radius of maximum wind (RMW) at flight level. All portions of the eyewall were well sampled, with some preference for the northeast (primarily right hand) quadrant, where the storm's strongest winds would be expected. A majority of sondes were released slightly inward of the flight-level RMW for the same reason; this fact will be an important consideration for the analysis in the next section. Most of the sondes were dropped from the 700-hPa level.

Each dropsonde profile was subjected to rigorous objective and subjective quality control (postprocessing) to ensure that any detectable errors were removed. Two aspects of the quality control are of interest here. First, to identify errors in the horizontal winds, the GPS-derived vertical sonde motions were compared with vertical fall rates determined hydrostatically from the pressure data. Occasional bad GPS winds (that result, for example, when one of the GPS satellites is misidentified) can easily be identified by discrepancies between the GPS and hydrostatic sonde fall rates. Second, the final sounding has a filter applied to eliminate aliasing of scales unresolvable by the 0.5-s sampling of the sonde (i.e., scales of ~3 s or less). (The sonde has a sampling interval of 0.5 s, whereas the time period over which any particular wind measurement is made by the GPS hardware is on the order of milliseconds.) The data used for this study were smoothed with a cutoff filter wavelength of 5 s, which corresponds to about 55 m in the vertical direction near the surface. This filtering only slightly reduces the sonde's depiction of very small scale turbulence or gustiness in the hurricane eyewall, as will be seen below.

3. Individual eyewall soundings

Individual dropsonde profiles from the hurricane eyewall reflect the turbulent environment through which

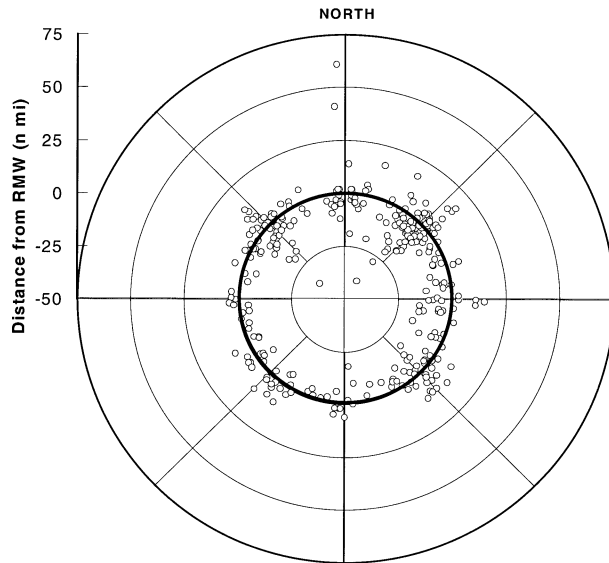


FIG. 2. Launch locations of eyewall dropsondes (open circles) relative to the location of the flight-level RMW. The RMW is indicated by the heavy circle, and the sonde locations are plotted in terms of distance inward or outward from the RMW.

the sondes fall. Figure 3 shows a profile made in the southeast quadrant of the eyewall of Hurricane Georges at 0008 UTC 20 September 1998. Winds are seen to be relatively constant from 3000 down to about 2000 m, at which point the speed generally increases, reaching a peak value of 177 kt (91 m s^{-1}) near 750 m in altitude.² This particular release was made about 6 n mi (11 km) inward of the flight-level RMW. Because the RMW in a tropical cyclone typically slopes inward with decreasing height (e.g., Jorgensen 1984), this sonde would have been gradually approaching the sloping RMW as it fell. Some of the wind increase seen between 3000 and 750 m, then, is due to eyewall slope rather than to a general increase in the storm's tangential wind. It must also be remembered that eyewall sondes may cover a significant distance azimuthally as they fall, and so the sonde does not provide a true vertical profile (downwind translations of 10° – 30° are typical during the 4 min or so it takes for a sonde to reach the surface from 700 hPa).

At least two distinct scales are apparent in the profile. A fairly broad maximum of wind speed is present from about 200 to 800 m in elevation. It took the sonde roughly 50 s to traverse this layer, and so it may be reasonable to interpret this broad maximum as a sustained, or mean wind. On the other hand, there are three shallow layers of significantly stronger winds superimposed on the broad maximum. These peaks are roughly 50 m deep and are sampled by the sonde for less than 5 s. Although

² The highest wind speed observed by a dropsonde in a hurricane is 192 kt (99 m s^{-1}), in Hurricane Kenna on 24 October 2002, at an altitude of about 116 m. Higher wind speeds, up to 215 kt (109 m s^{-1}), have been observed by dropsondes in the upper-tropospheric jet core during the winter season.

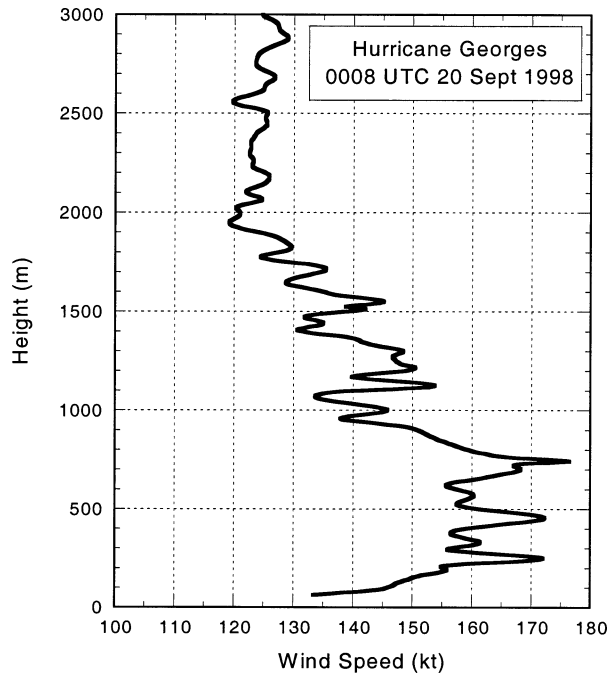


FIG. 3. Dropwindsonde wind speed profile from the eyewall of Hurricane Georges at 0008 UTC 20 Sep 1998.

one cannot determine the horizontal scale of these shallow features, it may be reasonable to interpret them as gusts. These interpretations presume that features of relatively deep vertical extent are also relatively large in azimuthal extent.

Hock and Franklin (1999) showed a pair of dropsonde profiles taken 6 s and 1 km apart over the Gulf of Mexico in January of 1998 (their Fig. 7). Over a depth of 8000 m, in winds of more than 20 m s^{-1} , these profiles tracked each other almost precisely, never deviating by more than 1 m s^{-1} . That kind of agreement is generally not seen in closely spaced hurricane soundings, but gross similarities between soundings are common. Figure 4 shows sets of closely spaced eyewall profiles from Hurricanes Bonnie and Mitch of 1998. The smaller-scale details vary considerably from sounding to sounding, but the Bonnie profiles all generally indicate relatively little speed shear between 3000 and 600 m and show a fairly large reduction in wind speed below 200–300 m. The Mitch profiles, on the other hand, show a general increase in wind from 3000 m nearly down to the surface layer, and, in fact, the surface winds in these profiles were higher than any flight-level wind observed over the 6-h period that the aircraft was in the storm. The Mitch profiles show a relatively high degree of small-scale “gustiness,” whereas the corresponding features in the Bonnie soundings are of smaller amplitude, suggesting a less turbulent, less convective environment.

Eyewall sondes closely spaced at launch tend to separate as they fall, in part because of the turbulent nature of the wind field and the extreme radial gradients in the

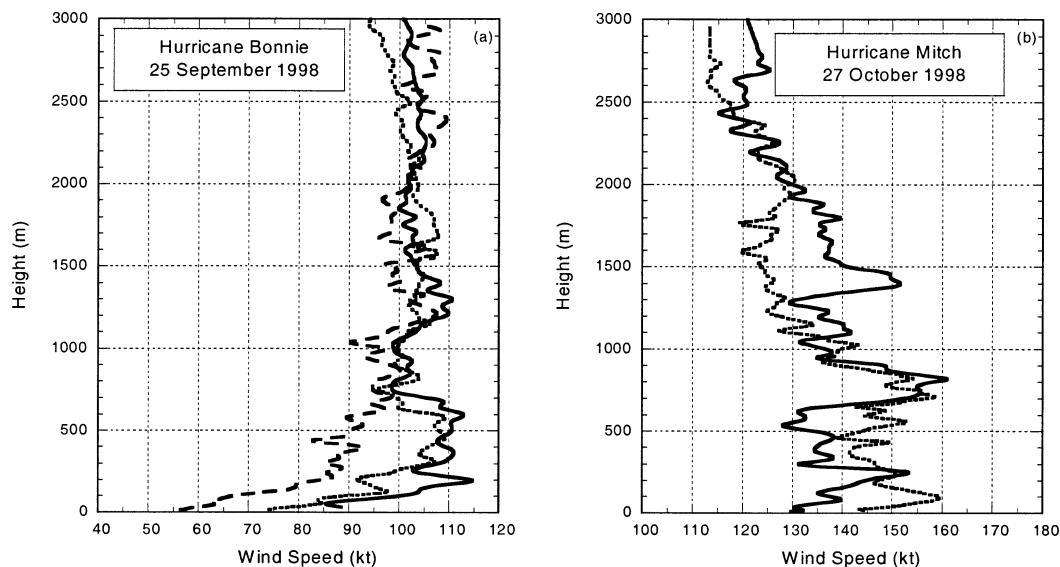


FIG. 4. Dropwindsonde profiles from the eyewall of (a) Hurricane Bonnie on 25 Sep 1998 and (b) Hurricane Mitch on 27 Oct 1998. The times of the profiles in (a) are 0015 (solid), 0017 (short dashes), and 0021 (long dashes) UTC. The times of the profiles in (b) are 2337 (solid) and 2343 (dashed) UTC.

eyewall. Figure 5 shows the trajectories of two sondes released near the inner edge of the eyewall of Hurricane Bret on 21 August 1999; the wind profiles from the two sondes are shown in Fig. 6. The first of the pair remains near the inner edge of the eyewall, with a profile characterized by relatively constant winds down to about 1200 m, followed by an increase at low levels. The strongest winds in this sounding are found within 150 m of the surface. The second sonde, on the other hand, is carried radially outward toward the stronger convection in the heart of the eyewall. Consistent with this trajectory, winds in this profile begin to increase at a higher altitude than the first. The strongest winds in the latter case are found near 700 m.

Given the frequent differences between nearly simultaneous releases and the amount of small-scale transient information present in individual eyewall profiles, it becomes clear that calculating the ratio of, say, the surface wind speed to the 700-hPa wind speed from any individual sounding is of little value. It also should be clear that a raw surface wind report from a dropsonde in a turbulent environment should not be considered necessarily to be representative of a sustained wind. However, by averaging large numbers of profiles together, a mean structure emerges from which useful empirical relationships can be determined.

4. Mean soundings and sample stratifications

a. Method

As noted earlier, each sounding was assigned to one of two categories: eyewall or outer vortex. This assignment was based on examination of individual flight-level radial wind profiles near the time of sonde launch

and, where available, airborne radar reflectivity imagery. Sondes released along the inner edge of the eyewall, such as those from Hurricane Bret shown in Figs. 5 and 6, were excluded from the dataset. For each eyewall sonde, an RMW was determined subjectively from the flight-level radial wind profile data, and the radial distance of the sonde from the flight-level RMW was calculated. When there were multiple wind maxima, the distance to the nearest one was used. Detailed storm tracks using all available aircraft center fixes were generated, so that storm-relative quantities could be calculated.

After each sounding was postprocessed to ensure quality control, wind values were extracted from the 2-Hz observations by interpolation, beginning at 10 m (the nominal surface level) and continuing at 5-m intervals to the launch altitude of that particular sounding. The individual interpolated soundings were used to construct a number of mean eyewall profiles for several stratifications of the dataset. Prior to averaging, the wind speed at each level in the drop profile was normalized by the wind speed at a reference level. Common reconnaissance flight levels [e.g., 700, 850, and 925 hPa and 1000 ft (305 m)] were used as reference levels, so that the resultant mean speed profiles would be expressed as a percentage of the wind speeds available to the operational forecasters. The normalization wind speed was taken from the dropsonde profile, if available, or from the aircraft flight-level wind, if the aircraft was at the reference altitude.

The maximum number of eyewall soundings reporting for any particular level was 404, at 950 m. The eyewall observation count for levels from 10 to 400 m is shown in Fig. 7. It can be seen that the number of

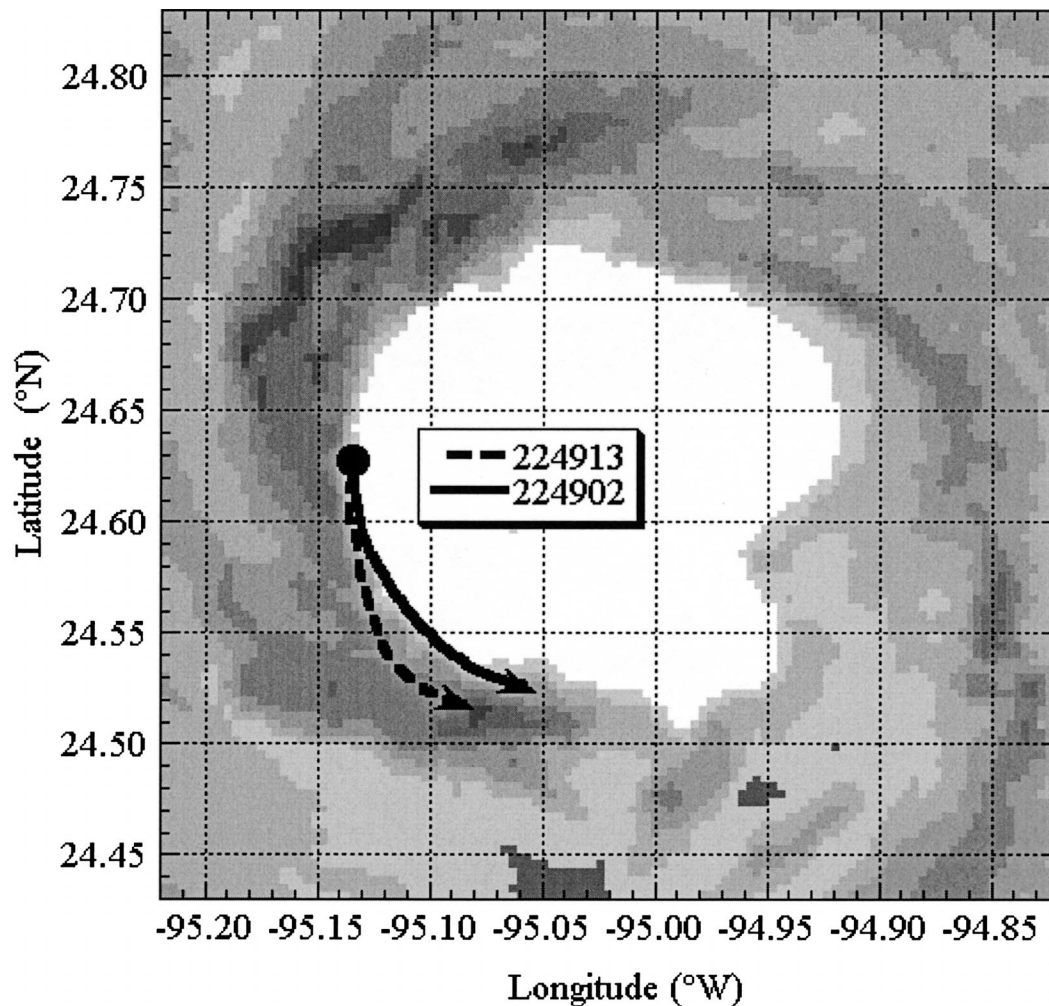


FIG. 5. Single-sweep radar reflectivity image, from an altitude of 4.3 km, of the eyewall of Hurricane Bret at 2254 UTC 21 Aug 1999, showing the launch location (black circle) and trajectories followed by two sondes released near the eyewall's edge. The release times [hhmmss (hour, minutes, seconds) UTC] of the two sondes are given in the legend. The dBZ scales are shown as increasing shades of gray, with thresholds at 15, 20, 25, 30, 35, 40, and 45 dBZ.

sondes reporting winds remained relatively constant down to about 100-m elevation, at which point increasing numbers of sondes began to fail. A second, sharper increase in failure rate is seen to occur near 30 m, such that only 172 of the 429 eyewall sondes reported a 10-m wind. The reasons for this phenomenon are not completely understood but are likely related to an inability of the GPS dropsonde receiver to track GPS satellites when the sonde undergoes extreme accelerations. Indeed, failure rates are higher in the strongest storms. Such an abrupt and systematic change in the dataset at 30-m elevation could, if unaccounted for, introduce an artificial discontinuity in the computed mean profiles. To prevent such a discontinuity, a separate mean profile over the 10–30-m layer was computed for those 172 eyewall sondes that reported continuously over this interval. For this sample, the mean ratio of 10–30-m wind speed was 0.925. In all of the eyewall results shown

below, regardless of how many sondes were available above the 30-m level, this 172-sonde homogeneous sample has been used to represent all changes in wind speed over the 10–30-m layer.

b. Mean wind speed profiles

Figure 8 shows the mean wind speed profile for the hurricane eyewall, in which the wind at each level has been normalized by the wind speed at 700 hPa. The mean eyewall 700-hPa height was near 2900 m (where the normalized wind speed is equal to 1). The result of primary interest to forecasters is the ratio of the eyewall surface to 700-hPa wind speed (R_{700}), which from the figure is seen to be 0.91. The strongest winds (presumably representing the top of the boundary layer) in the eyewall are found near 500-m elevation, a somewhat lower level than is typically suggested by Doppler radar

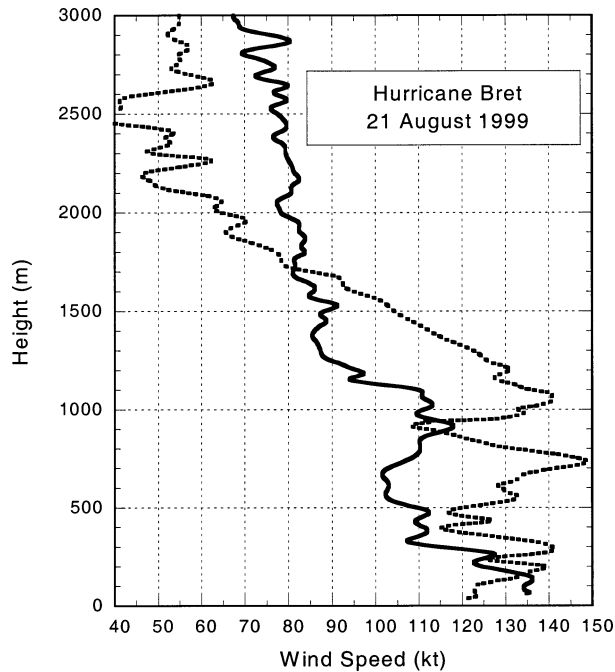


FIG. 6. Dropwindsonde profiles from the eyewall of Hurricane Bret on 21 Aug 1999. The times of the profiles are 2249:02 (solid curve) and 2249:13 (dashed curve) UTC.

case studies (e.g., Marks and Houze 1987; Marks et al. 1992). The mean profile shows that the peak winds near 500 m are about 20% higher than the 700-hPa wind, owing to the warm-core nature of the tropical cyclone, although this effect is in fact slightly overstated here because of a sampling bias, as will be shown below. Below 300 m, in the frictional boundary layer, there is a sharp reduction of wind speed that is nearly logarithmically linear (Fig. 9).

For comparison, mean profiles are also shown in Figs. 8 and 9 for the outer vortex, that is, the area outside the eyewall but within 300 km of the cyclone center. In the outer vortex, the low-level wind maximum is found just below 1 km, at a somewhat higher elevation than in the eyewall, and its magnitude is not nearly as pronounced; the peak winds are only about 10% stronger than the 700-hPa winds. Again, the profile is nearly logarithmically linear below 300 m. The ratio of surface to 700-hPa wind speed is 0.78, lower than in the eyewall. These results are in good agreement with earlier hurricane studies that had scant access to eyewall observations, such as Powell and Black's (1990) estimate of $R_{700} = 0.73$ for unstable conditions. The height of the wind speed maximum found here is also in good agreement with earlier rawinsonde-based studies of the outer vortex (Miller 1958; Izawa 1964).

As noted earlier, a sonde that is released at a location radially inward of the flight-level RMW will approach the sloping RMW as it falls. Therefore, a portion of the measured increase in winds as the sonde descends is not "real," in the sense that it is not representative of

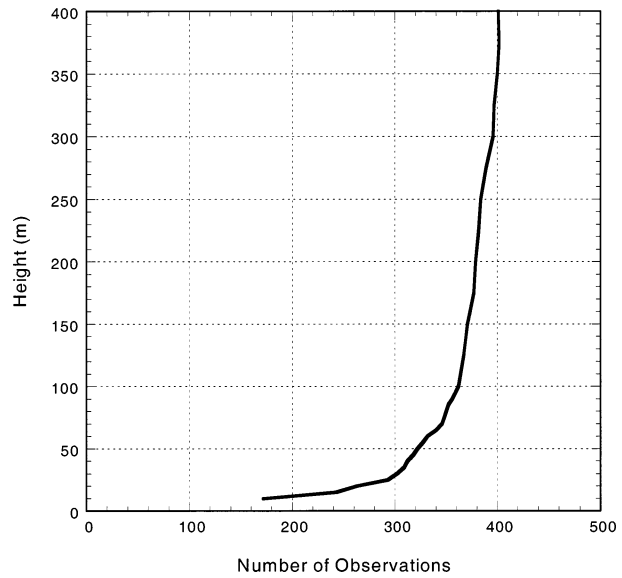


FIG. 7. Number of eyewall dropsondes that reported winds, as a function of elevation.

the true variation of the hurricane's *maximum* wind with height. Because a majority of the eyewall dropsondes were released inward of the flight-level RMW (Fig. 2), the previous estimate of $R_{700} = 0.91$ could have a high bias. To convert peak 700-hPa reconnaissance winds to

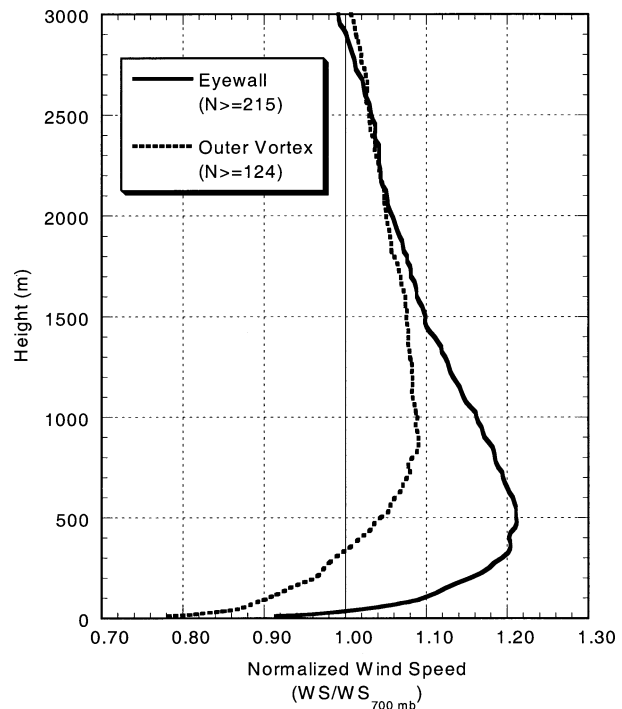


FIG. 8. Mean hurricane wind speed profiles for the eyewall and outer-vortex regions. Wind speeds are averaged and expressed as a fraction of the profile wind speed at 700 hPa. The minimum number of profiles used to construct the averages is also indicated.

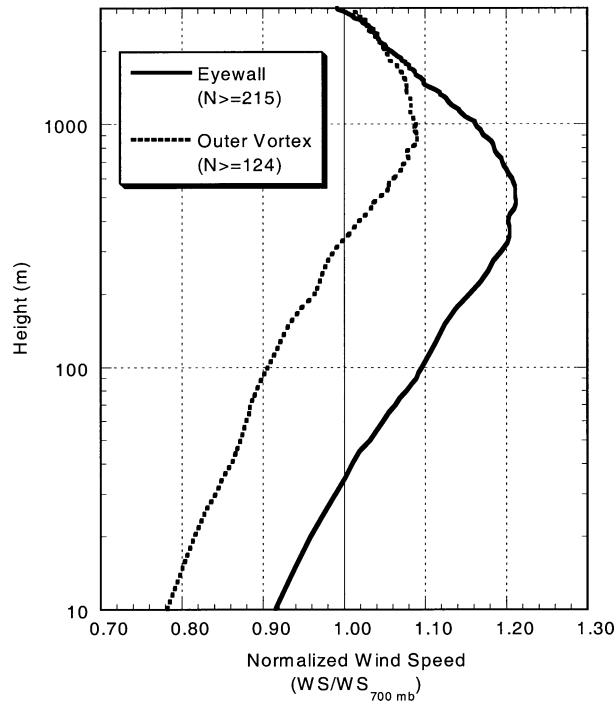


FIG. 9. As in Fig. 8 except that the height axis is plotted on a logarithmic scale.

peak surface winds in a tropical cyclone, what is needed is the value of R_{700} along the sloping RMW. A lower bound on this value can be determined from a mean eyewall profile valid at the *flight-level* RMW, for, in this case, the flight-level wind is maximized while the sonde is now moving away from the RMW as it falls.

Figure 10 shows three mean eyewall profiles, constructed by stratifying the sample by distance from the RMW. As expected from the preceding discussion, it can be seen that there is significantly less speed shear in the outer portion of the eyewall than in the inner portion. For those sondes released closest to the flight-level RMW (the solid line), the profile shows the peak winds are about 17% higher than the 700-hPa wind speed, and the ratio $R_{700} = 0.88$.

Because this value $R_{700} = 0.88$ was obtained at the flight-level RMW, the “true” value of R_{700} , that is, the value appropriate for converting peak 700-hPa reconnaissance winds in the eyewall to peak surface winds, should lie between 0.88 and the 0.91 estimate arrived at previously. Thus, at least in the mean, these data confirm the validity of NHC’s operational practice of using adjustment factors higher than those recommended by Powell and Black (1990) for the conversion of 700-hPa aircraft reconnaissance data to the surface. In fact, the adjustment factors in use during much of the 1990s (predominantly in the 80%–90% range) will, in many cases, have been low.

Reconnaissance aircraft may conduct their missions at one of several altitudes, generally flying higher for

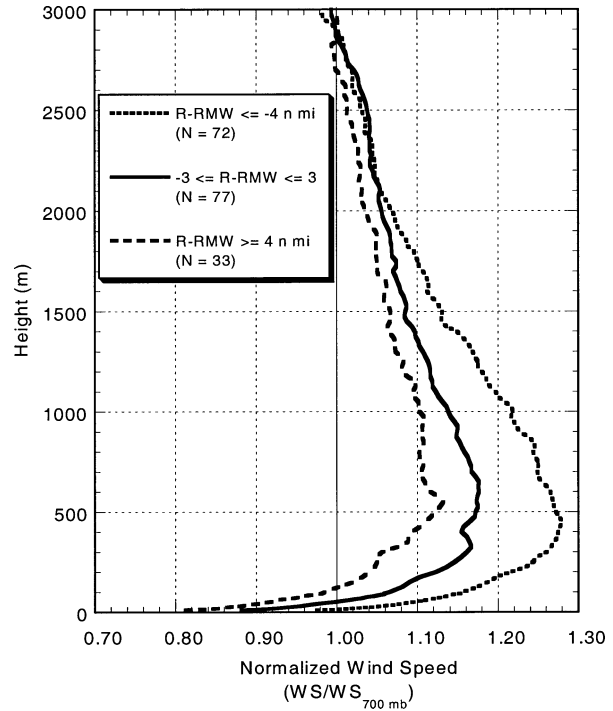


FIG. 10. Mean wind speed profiles for eyewall sondes released within 3 n mi (5.6 km) of the flight-level RMW (solid line), for eyewall sondes released at least 4 n mi (7.4 km) radially outward of the RMW (long dashed line), and for eyewall sondes released at least 4 n mi (7.4 km) radially inward of the RMW (short dashed line). All winds are averaged and are expressed as a percentage of the profile 700-hPa wind speed.

safety reasons in the stronger storms. The above analysis was repeated to determine recommended operational adjustment factors for each of the common flight altitudes, and these results are summarized in Table 2. Although flight altitude has only infrequently been considered in the past in determining hurricane winds, the mean profiles determined by the dropsonde data clearly show that this factor should be taken into account. For determining a tropical cyclone’s maximum surface winds, the recommended surface-to-flight-level wind ratios are 0.9, 0.8, and 0.75, for adjustments from 700, 850, and 925 hPa, respectively.

In addition to the maximum winds, forecasters also are currently charged with estimating the radial extent of 64-, 50-, and 34-kt winds (33, 26, and 17 m s⁻¹,

TABLE 2. Recommended operational wind adjustment factors for adjusting reconnaissance flight-level winds to the surface, for the hurricane-eyewall and outer-vortex regions.

Flight level	Eyewall	Outer vortex (convection)	Outer vortex (not in convection)
700 hPa	0.90	0.85	0.80
850 hPa	0.80	0.80	0.75
925 hPa	0.75	0.75	0.75
1000 ft (305 m)	0.80	0.80	0.80

respectively) in each of four quadrants around the storm. Thus, surface wind adjustment factors outside of the eyewall are also of interest and are included in Table 2 to help forecasters in their determination of outer wind radii. For a subset of about 70 outer vortex sondes in this study, airborne radar reflectivity data were available to determine whether these sondes were released within or outside of convective areas, using a threshold of 30 dBZ to separate the two classes. Separate adjustment factors were determined for each group. Although not conclusive because of the limited sample, there appeared to be some differences in adjustment factors for the higher altitudes. For example, R_{700} was found to be 0.78 for the complete outer vortex sample of ~ 200 sondes. However, from the smaller sample of 70 sondes that could be assigned to the convective or nonconvective categories, R_{700} was found to be 0.87 and 0.78, respectively, leading to the (rounded) recommendations in Table 2. In an operational setting, satellite imagery could be used subjectively to characterize the various quadrants around the storm as either convective or nonconvective.

c. Variation of mean profiles and surface wind adjustment factors

As noted earlier, the structure of individual profiles is affected by the precise release location as well as by what small-scale variability is encountered by chance. The standard deviation of R_{700} about its mean eyewall value of 0.9 is very high (~ 0.19). Nevertheless, a storm's "character" tends to emerge after a number of eyewall soundings are obtained. Figure 11 shows mean profiles computed for the more thoroughly sampled hurricanes. Different shapes are readily apparent. For example, note the differences between the mean profiles for Lenny and Bret. Bret's low-level wind maximum was relatively narrow and peaked, with significant speed shear above the boundary layer; Lenny's was broad, with little speed shear aloft. It is significant that the operational dropsonde data indicated that Bret's surface winds had reached category-4 intensity on the Saffir-Simpson hurricane scale (Simpson 1974) about 12 h before such strengthening became apparent in the 700-hPa flight-level observations. Hurricane Bonnie is notable for a low-level wind maximum that is fairly broad and relatively high (in elevation) and for its relatively low surface-to-700-hPa wind ratios. Of the storms sampled thus far, Bonnie had the lowest mean R_{700} (0.83). The highest storm-averaged R_{700} was observed in Dennis (0.97). This latter ratio is probably not quite representative, because the Dennis sondes tended to be dropped more radially inward than most; however, R_{700} was 0.93 for those Dennis sondes located within 3 n mi of the RMW. Of course, such ratios evaluated locally can be much higher or lower.

Additional stratifications of the sample have been performed to determine what factors are related to the var-

iability of the eyewall profile shape and the surface adjustment factors. Figure 12 shows how the eyewall profile shape in the boundary layer varies as a function of wind speed. The figure shows normalized wind speed profiles, as before, but here the profiles have been normalized by the mean wind over the 300–700-m layer. Because this layer is near the peak of the mean profile, the diagram shows how effectively the hurricane eyewall's strongest winds are being transported to the surface, while it avoids sampling issues related to eyewall slope at higher altitudes. The data have been grouped into six bins based on the mean wind speed in the normalization layer.

It is seen that there is relatively little drop-off of wind speed in the boundary layer when the winds are low ($20\text{--}30\text{ m s}^{-1}$) and that as the wind near the top of the boundary layer increases to $40\text{--}50\text{ m s}^{-1}$ the fraction of that wind penetrating downward decreases. This behavior is predicted by boundary layer models that have traditionally been used to adjust hurricane winds (e.g., Powell 1980). However, the dropsonde data show that this trend reverses as the wind speed increases further, in contrast to the behavior of the boundary layer models. Note that by the time the wind near the boundary layer top has increased to $70\text{--}80\text{ m s}^{-1}$, the fraction of that wind reaching the surface has increased to nearly the same value it had when the winds were $20\text{--}30\text{ m s}^{-1}$. Given the relatively small sample size at the highest wind speeds, however, this result is not conclusive.

It has been suggested (M. D. Powell 2001, personal communication) that these increased surface winds (in a relative sense) in the stronger storms may be due to physical changes to the air-sea interface that are effectively reducing frictional effects at extreme wind speeds. The apparent change in slope between the $60\text{--}70$ and $70\text{--}80\text{ m s}^{-1}$ mean profiles below about 200 m is suggestive of this effect. Recalling that a uniform profile reduction at all wind speeds was imposed over the $10\text{--}30\text{-m}$ layer, one suspects that this effect may even be a little larger than indicated here.

One can also speculate that enhanced vertical transports of momentum in the stronger storms are resulting in higher surface wind adjustment factors (Black and Franklin 2000). Indeed, it has long been the practice at NHC to consider the degree of convective activity in the interpretation of reconnaissance flight-level observations (Sheets 1990). Because the dropsondes are capable of measuring vertical motions, this possibility can be investigated further.

The GPS receiver in the dropsonde essentially measures the three-dimensional displacement of the sonde. The horizontal displacement is the horizontal wind, and the vertical displacement represents the combination of the vertical wind and the "still air" fall rate of the dropsonde, which is a function of the sonde weight, parachute characteristics, and air density. The vertical wind can therefore be computed as the difference between the sonde's actual and theoretical still-air fall

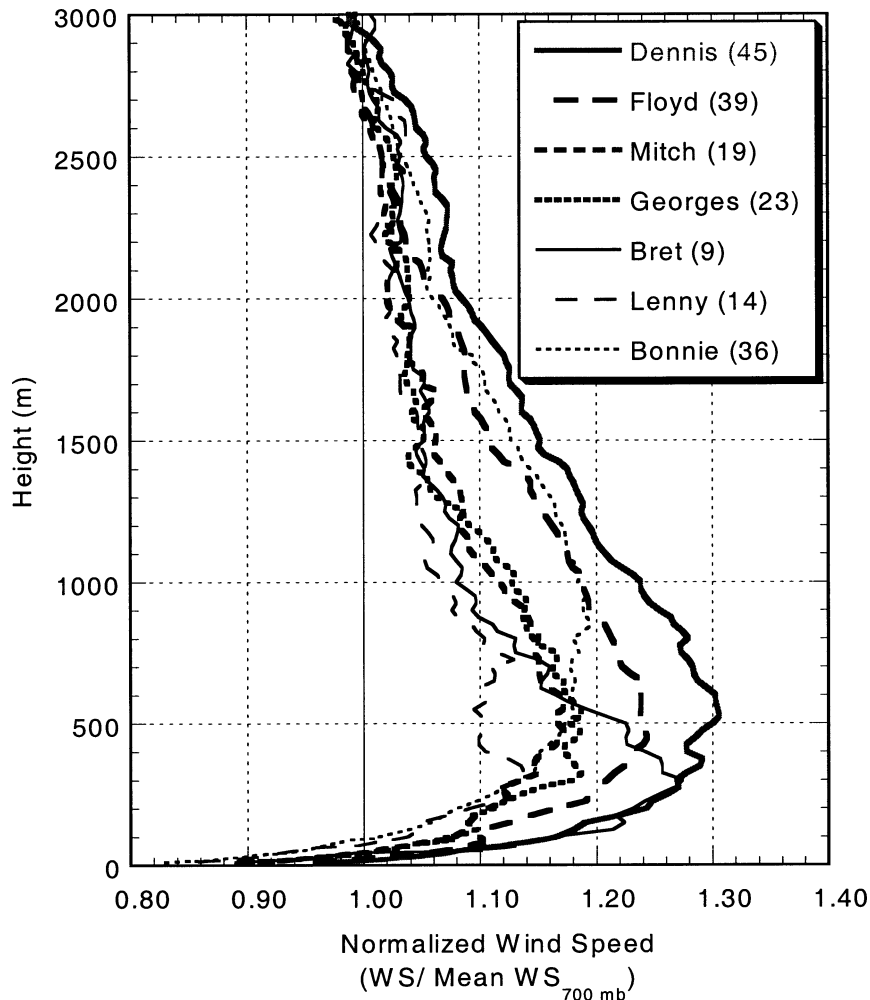


FIG. 11. Mean eyewall wind speed profiles for individual hurricanes. All winds are averaged and are expressed as a percentage of the profile 700-hPa wind speed. The number of soundings used to construct the mean profile for each storm is given in parentheses in the figure legend.

rates. Factors such as manufacturing variations among parachutes can introduce errors in the computed vertical winds. Based on examination of several thousand vertical wind speed soundings, the absolute uncertainty of these computations is believed to be about $0.5\text{--}1.0\text{ m s}^{-1}$; however, the relative errors in vertical velocity within a single sounding should be considerably less. Vertical motions determined in this fashion tend to correlate well with features visible in the sondes' thermodynamic data (Hock and Franklin 1999).

For each of the eyewall soundings, the mean absolute vertical velocity (i.e., without regard to sign) was computed over the layer from the surface to 2000 m to get an overall measure of convective activity. Each sounding was then assigned to a bin based on its mean vertical velocity (either $0.0\text{--}0.5$, $0.5\text{--}1.0$, $1.0\text{--}1.5$, $1.5\text{--}2.0$, or $2.0\text{--}3.0\text{ m s}^{-1}$), and mean adjustment factors were determined for each bin. The results are shown in Fig. 13 and indicate that, when vertical motions are more vig-

orous, a larger fraction of the eyewall flight-level wind is present at the surface. As might be expected, it is the downdrafts below the level of maximum wind that are responsible, as illustrated in Fig. 14. Here, the signed (not absolute) value of the vertical velocity is averaged over the lowest 250 m of the sounding and is divided into 1 m s^{-1} wide bins over the range from $+1.5$ to -2.5 m s^{-1} . The figure shows that low-level updrafts are associated with relatively low surface winds and that the low-level downdrafts are associated with higher surface winds.

5. Operational considerations

Individual dropsonde profiles contain information on a variety of scales. Because the sonde responds to whatever turbulence it encounters as it descends, "spot" values at any given level should not be interpreted as a sustained (e.g., 1-min mean) wind. Turbulence studies

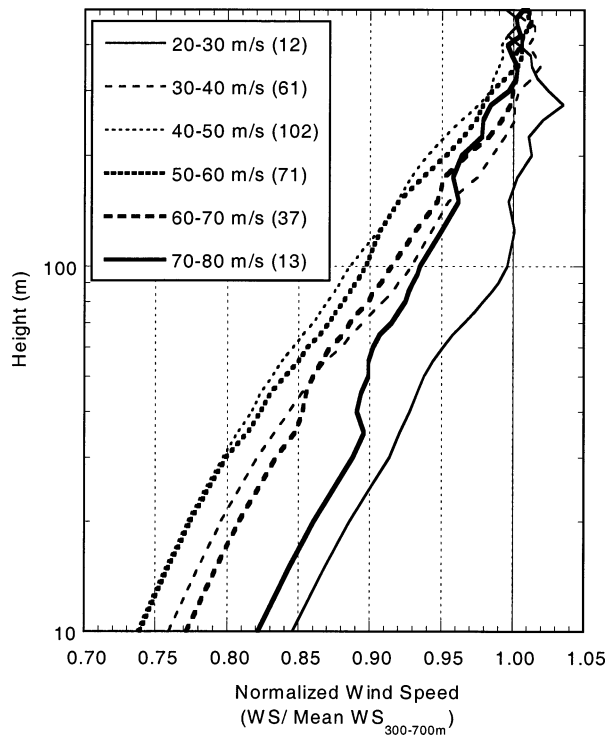


FIG. 12. Mean boundary layer eyewall wind speed profiles for various ranges of average wind speed in the 300–700-m layer. All winds are averaged and are expressed as a percentage of the profile 300–700-m-layer-mean wind speed. The number of soundings used to construct the mean profile for each storm is given in parentheses in the figure legend.

have demonstrated that Lagrangian (parcel) wind measurements are inherently smoother than Eulerian (fixed-point anemometer) measurements (Gifford 1955), with dominant periods longer by a factor of about 3–4 (Angell et al. 1971). This result can be understood by considering an air parcel representing a gust as it moves past an anemometer. From the anemometer’s point of view, the gust parcel moves quickly past the instrument and is gone, whereas a tracer embedded within the gust continues to experience the higher wind speed for an extended period of time. This would suggest that a parcel trajectory would in general require very long averaging times, on the order of several minutes, to obtain something equivalent to a 1-min mean anemometer wind. Such averaging is, of course, not possible with a dropsonde, which samples the wind at any given level only briefly.

In light of these data and considerations, two layer-averaged winds, along with the actual measured 10-m dropsonde wind, are currently considered by the NHC. A relatively conservative estimate of the surface wind is obtained by averaging the dropsonde wind speed over the 0–500-m layer, or roughly the depth of the boundary layer. This mean boundary layer (MBL) wind speed is then multiplied by 0.80, the mean ratio of the 10-m speed to the MBL speed determined from the sample

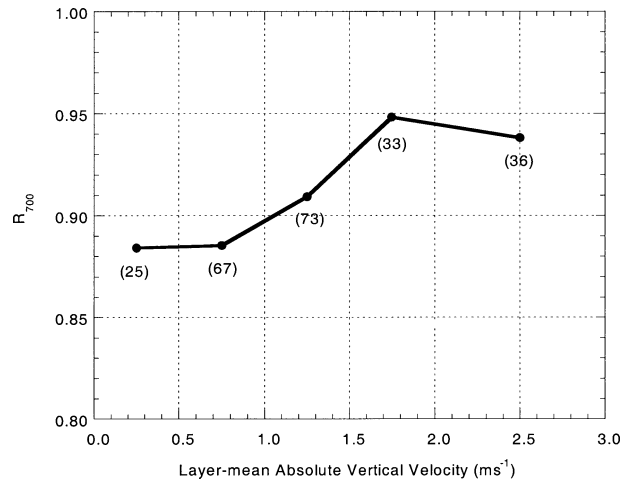


FIG. 13. Surface-to-700-hPa wind speed ratio R_{700} as a function of sounding-mean absolute vertical velocity, in which the absolute vertical velocity is averaged over the layer from the surface to 2000 m. The number of soundings used to construct each bin average of R_{700} (see text) is shown in parentheses.

of eyewall dropsondes. The resulting surface wind estimate has the advantage of having an averaging time close to 1 min (~ 45 s) but has the disadvantage of treating all storms alike. Therefore, a second average is calculated over the lowest available 150 m of the dropsonde profile. This low-layer-mean wind (denoted as “WL150” in the transmitted dropsonde message) is then adjusted to the surface using the dropsonde-based mean eyewall profile. This latter estimate is better able to represent a storm’s particular character, at the potential risk of being less representative of the sustained wind. In operational use, if repeated eyewall dropsondes show a systematic difference between the MBL- and WL150-

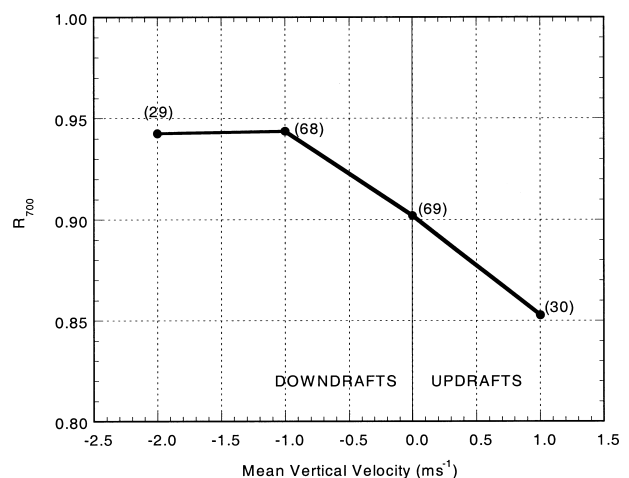


FIG. 14. Surface-to-700-hPa wind speed ratio R_{700} as a function of sounding-mean vertical velocity, in which the vertical velocity is averaged over the layer from the surface to 250 m. The number of soundings used to construct each bin average of R_{700} (see text) is shown in parentheses.

TABLE 3. Mean wind speed in the hurricane eyewall, expressed as a fraction of the surface wind speed, as a function of altitude. corresponding building heights in stories are also given, assuming an average of one story for every 10 ft (3.05 m) of elevation. The wind pressure force on an object is proportional to the square of the wind speed.

Altitude (m)	Stories	Wind (% of the surface value)	Pressure force (% of surface value)
10	3	100.0	100.0
15	5	102.7	105.5
20	6	104.8	109.7
30	10	108.1	116.9
50	16	112.8	127.2
75	25	116.9	136.5
100	33	119.8	143.5
150	49	122.9	151.0
200	66	126.1	159.1
250	82	128.8	165.8
300	98	130.5	170.3

based surface wind estimates, then more weight is given to the latter.

Two factors that likely are related to the eyewall profile structure are wind speed and vertical motion. A minimum in the surface wind adjustment factor was found when the wind near the top of the boundary layer was between 40 and 60 m s⁻¹. At higher speeds, the fraction of the boundary layer wind speed found at the surface increased, contrary to expectation. Low-level downdrafts, and enhanced vertical motion generally, were associated with higher relative surface winds. From an operational perspective, a forecaster might want to use an adjustment factor slightly higher or lower than the recommended values for storms that had unusually vigorous or anemic convection, respectively.

One would expect there to be a relationship between surface wind ratios and sea surface temperature; actual SSTs were unfortunately not available for this study. Only a weak relationship was found between R_{700} and climatological SSTs, over the range of 22°–29°C. In addition, there were only modest differences in R_{700} between the left and right sides of the hurricane eyewall, with R_{700} in the left quadrant about 4% higher than in the right quadrant—a difference not large enough to change the recommended adjustment factors given in Table 2. In the outer vortex, right–left differences were larger (again, with the lower values of R_{700} on the right side, consistent with a steering level in the midtroposphere), but the outer vortex sample is too limited to consider this result to be conclusive.

The dropsonde profiles may be of interest to engineers concerned with building codes, to emergency managers who may be tempted to use high-rise buildings as a “refuge of last resort” in coastal areas, and to hurricane-prone populations at elevated terrain. The dropsonde results are strictly valid only over the water, but they should be approximately valid at the immediate coastline as well, at least on the right-hand side of landfalling storms. Table 3 expresses the mean eyewall profile’s

variation with altitude as a percentage of the surface wind (the wind contained in NHC advisories). For example, based on the mean eyewall profile, a 25-story coastal high-rise in the hurricane eyewall will experience a sustained wind about 17% higher (or one Saffir–Simpson hurricane-scale category) than the surface or advisory value. The top of a 50-story building will experience sustained winds about 23% higher (and a pressure force 50% higher) than at the surface. Of course, in individual storms the increase in winds with height could be higher or lower. Because the actual standards employed in the construction of particular buildings are generally not known, residents who must take refuge in coastal high-rises should do so at the lowest levels necessary to avoid storm surge. The engineering community is invited to evaluate building codes in hurricane-prone areas against the dropsonde-based hurricane wind profile.

6. Summary

The recent development of the GPS dropwindsonde has allowed the wind structure of the hurricane eyewall to be documented with unprecedented accuracy and resolution. In the first three years of its availability, a sample of over 400 soundings was obtained from the eyewalls of 17 hurricanes, with an additional ~200 hurricane soundings made outside of the eyewall but within about 300 km of the center. In an attempt to assist operational hurricane forecasters in their duties, we have used the dropwindsonde data to document, for the first time, the mean inner-core vertical wind structure of a hurricane from the surface to the 700-hPa level (the level typically flown by reconnaissance aircraft).

The dropsonde-derived mean eyewall wind profile is characterized by a broad maximum centered 500 m above the surface. Above this maximum, the winds decrease because of the hurricane’s warm core, with the peak winds nearly 20% higher than the 700-hPa wind speed. Below the level of maximum wind, speeds decrease in the frictional boundary layer nearly linearly with the logarithm of the altitude, with the surface (10 m) wind being approximately 75% of the peak value. These two effects combine to give a surface wind that is, on average, about 90% of the 700-hPa value. Thus, claims of inflated NHC maximum sustained surface wind estimates are not supported by the dropwindsonde observations; in fact, because NHC has used surface wind adjustment factors over the past decade generally in the range of 80%–90%, a number of storms probably had their intensities underestimated. (The recent adjustment of the official intensity of 1992’s Hurricane Andrew, from 125 to 145 kt at its south Florida landfall, was based largely on the new dropsonde-derived adjustment factors.) The current results differ from earlier studies primarily because of the heretofore limited quantity and quality of observations from the hurricane eyewall. In particular, the decrease in wind speed above the

boundary layer in the eyewall is larger than was previously assumed.

Acknowledgments. The authors gratefully acknowledge the dedicated crews and scientists of the NOAA Hurricane Research Division and Aircraft Operations Center (AOC) and also the 53d Weather Reconnaissance Squadron (WRS) of the Air Force Reserve Command, who endured considerable hardship in the collection of the data used in this study. In particular, Jeffrey Smith's efforts to ensure the quality of the dropwindsonde stocks are greatly appreciated. A special thanks is owed to Lee Weiher, Mike Scaffidi, and Scott Persinger of the 53d WRS for providing the AFRC observations and to Hal Cole, Terry Hock, and Dean Lauritsen of the National Center for Atmospheric Research, the leaders of the team that developed the GPS dropwindsonde. Dan Jimenez assisted in the tabulation of aircraft wind data. Partial funding of this research was provided by a grant from the U.S. Weather Research Program.

REFERENCES

- Angell, J. K., D. H. Pack, W. H. Hoecker, and N. Delver, 1971: Lagrangian–Eulerian time-scale ratios estimated from constant volume balloon flights past a tall tower. *Quart. J. Roy. Meteor. Soc.*, **97**, 87–92.
- Black, M. L., and J. L. Franklin, 2000: GPS dropsonde observations of the wind structure in convective and non-convective regions of the hurricane eyewall. Preprints, *24th Conf. on Hurricanes and Tropical Meteorology*, Fort Lauderdale, FL, Amer. Meteor. Soc., 448–449.
- Frank, W. M., 1977: The structure and energetics of the tropical cyclone. I. Storm structure. *Mon. Wea. Rev.*, **105**, 1119–1135.
- Franklin, J. L., and P. R. Julian, 1985: An investigation of Omega windfinding accuracy. *J. Atmos. Oceanic Technol.*, **2**, 212–231.
- , M. L. Black, and K. Valde, 2000: Eyewall wind profiles in hurricanes determined by GPS dropwindsondes. Preprints, *24th Conf. on Hurricanes and Tropical Meteorology*, Fort Lauderdale, FL, Amer. Meteor. Soc., 446–447.
- Gifford, F., Jr., 1955: A simultaneous Lagrangian–Eulerian turbulence experiment. *Mon. Wea. Rev.*, **83**, 293–301.
- Hawkins, H. F., and D. T. Rubsam, 1968: Hurricane Hilda, 1964: II. Structure and budgets of the hurricane on October 1, 1964. *Mon. Wea. Rev.*, **96**, 617–636.
- Hock, T. F., and J. L. Franklin, 1999: The NCAR GPS dropwindsonde. *Bull. Amer. Meteor. Soc.*, **80**, 407–420.
- Izawa, T., 1964: On the mean wind structure of typhoon. Tech. Note 2, Typhoon Research Laboratory, Meteorological Research Institute, Tokyo, Japan, 19 pp. [Available from NOAA/TPC Library, 11691 SW 17th St., Miami, FL 33165.]
- Jorgensen, D. P., 1984: Mesoscale and convective scale characteristics of mature hurricanes. Part II: Inner core structure of Hurricane Allen (1980). *J. Atmos. Sci.*, **41**, 1287–1311.
- Marks, F. D., Jr., and R. A. Houze Jr., 1987: Inner core structure of Hurricane Alicia from airborne Doppler radar observations. *J. Atmos. Sci.*, **44**, 1296–1317.
- , —, and J. F. Gamache, 1992: Dual-aircraft investigation of the inner core of Hurricane Norbert. Part I: Kinematic structure. *J. Atmos. Sci.*, **49**, 919–942.
- Miller, B. I., 1958: The three-dimensional wind structure around a tropical cyclone. NHRP Rep. 15, 41 pp. [Available from NOAA/TPC Library, 11691 SW 17th St., Miami, FL 33165.]
- Powell, M. D., 1980: Evaluations of diagnostic marine boundary layer models applied to hurricanes. *Mon. Wea. Rev.*, **108**, 757–766.
- , and P. G. Black, 1990: The relationship of hurricane reconnaissance flight-level wind measurements to winds measured by NOAA's oceanic platforms. *J. Wind Eng. Ind. Aerodyn.*, **36**, 381–392.
- Sheets, R. C., 1990: The National Hurricane Center—past, present, and future. *Wea. Forecasting*, **5**, 185–232.
- Simpson, R. H., 1974: The hurricane disaster potential scale. *Weatherwise*, **27** (8), 169, 186.
- Willoughby, H. E., J. A. Clos, and M. G. Shoreibah, 1982: Concentric eye walls, secondary wind maxima, and the evolution of the hurricane vortex. *J. Atmos. Sci.*, **39**, 395–411.